



Identification and synthesis of substituted pyrrolo[2,3-*d*]pyrimidines as novel firefly luciferase inhibitors

Yang Liu^{a,†}, Jianping Fang^{b,†}, Haiyan Cai^c, Fei Xiao^b, Kan Ding^{b,*}, Youhong Hu^{a,*}

^a State Key Laboratory of Drug Research, Shanghai Institute of Materia Medica, Chinese Academy of Sciences, Shanghai 201203, China

^b Glycochemistry & Glycobiology Lab, Shanghai Institute of Materia Medica, Chinese Academy of Sciences, Shanghai 201203, China

^c Drug Discovery and Design Center, Shanghai Institute of Materia Medica, Chinese Academy of Sciences, Shanghai, 201203, China

ARTICLE INFO

Article history:

Received 4 February 2012

Revised 21 July 2012

Accepted 21 July 2012

Available online 28 July 2012

Keywords:

Luciferase

Inhibitor

Pyrrolo[2,3-*d*]pyrimidine

High-throughput screening

Molecular docking

ABSTRACT

A novel firefly luciferase inhibitor (**3a**) with a pyrrolo[2,3-*d*]pyrimidine core was identified in a cell-based NF- κ B luciferase reporter gene assay. It potently inhibited the firefly luciferase derived from *Photinus pyralis* with an IC₅₀ value of 0.36 ± 0.05 μ M. Kinetic analysis of **3a** inhibition showed that it is predominantly competitive with respect to D-luciferin and uncompetitive with respect to ATP. Therefore, several pyrrolo[2,3-*d*]pyrimidine analogues were prepared to further investigate the structure-activity relationship (SAR) for luciferase inhibition. The most potent inhibitor of this series was **4c**, which showed an IC₅₀ value of 0.06 ± 0.01 μ M. In addition, molecular docking studies suggested that both **3a** and **4c** could be accommodated in the D-luciferin binding pocket, which is expected for a predominantly competitive inhibitor with respect to D-luciferin.

© 2012 Elsevier Ltd. All rights reserved.

1. Introduction

One of the most thoroughly studied oxidative enzymes is firefly luciferase, which is responsible for bioluminescence in firefly.^{1–3} It catalyzes two substrates (D-luciferin and ATP) to produce an enzyme-bound intermediate known as D-luciferyl-adenylate; this intermediate is oxidized, decarboxylated and converted to a singlet excited state of oxyluciferin (Scheme 1).² The spontaneous decay of oxyluciferin from the excited state to the ground state results in the release of photons that emit a yellow–green light (562 nm) at a pH of 7.5–7.8. The complicated reaction kinetics, production inhibition, and side competing dark reactions result in a typical light flash profile of the in vitro bioluminescence.^{2,4,5}

Due to its high sensitivity and convenience, firefly luciferase was widely used as the analytical tool for the quantification of ATP and the monitoring of pyrophosphatase activity in molecular biology only once after its isolation and purification.^{1,2,6} The successful cloning of the firefly luciferase gene in 1985 allowed firefly luciferase to be employed as a reporter gene in diverse applications, especially in the drug discovery area.^{7,8} Currently, bioluminescence assays based on luciferase enzymes are prevalent in high-throughput screening (HTS) assays and represent approxi-

mately 21% of all of the biochemical and cellular HTS assays performed today.^{9–12}

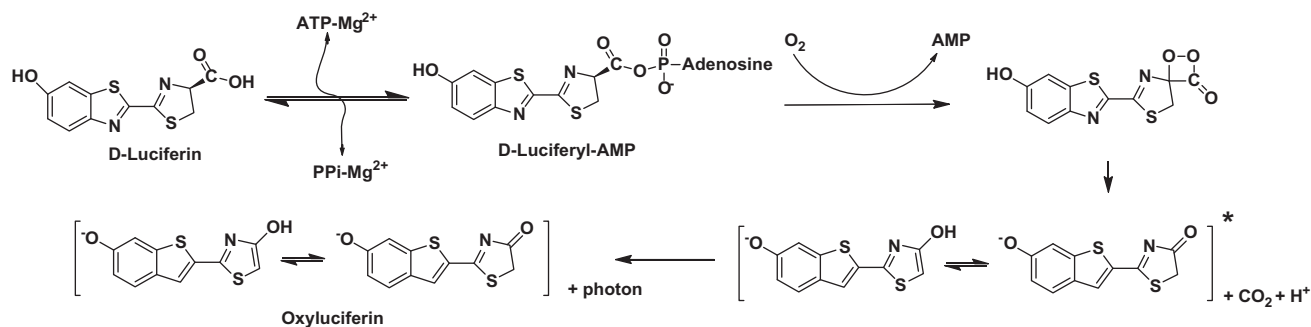
However, an important consideration in any assay that uses firefly luciferase as a reporter or a detection component is the inhibition of the enzyme by a variety of low-molecular-weight heterocyclic compounds, which are typically found in screening collections.¹³ This will lead to screening artifacts that are not attributed to modulating the biological activity or signal pathway of interest but may interfere with the interpretation of assay results.¹¹ Therefore, it is of utmost importance to eliminate these artifacts in the early HTS stages of drug discovery to save time, money, and identify artifacts as false positives.

Although firefly luciferase has a broad range of applications, many problems about its bioluminescence, such as the exact mechanism of luciferase's action in the reaction, are still not completely clear until now.² There is great interest in the identification and characterization of novel luciferase inhibitors to solve these problems to aid in the successful application and comprehension of luciferase. Moreover, a better understanding of luciferase inhibitors could shed light on ways to target other oxygenases that may be relevant to human health, such as cytochrome p450, cytochrome c, and monoamine oxidase.^{14–17} Furthermore, due to their structural similarities, firefly luciferase has been proposed as a model for the μ -opioid receptor,¹⁸ and thus some luciferase inhibitors might also have analgesic effects. Several different classes of small molecules that block luciferase activity have been identified, including substrate-related compounds, intermediates or products of the luciferase catalyzed reactions,^{19–21} anesthetics, certain fatty

* Corresponding authors. Address: 555 Zuchongzhi Road, Zhangjiang High-Tech Park, Shanghai, China. Fax: +86 2150806928 (K.D.); +86 2150805896 (Y.H.).

E-mail addresses: kding@mail.shnc.ac.cn (K. Ding), yhhu@mail.shnc.ac.cn (Y. Hu).

† Both authors contributed equally to this study.



Scheme 1. Schematic representation of luciferase catalyzed reaction.

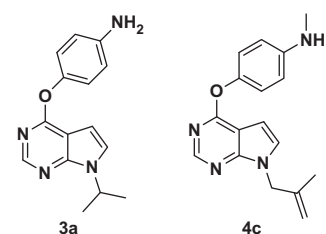


Figure 1. The novel luciferase inhibitors.

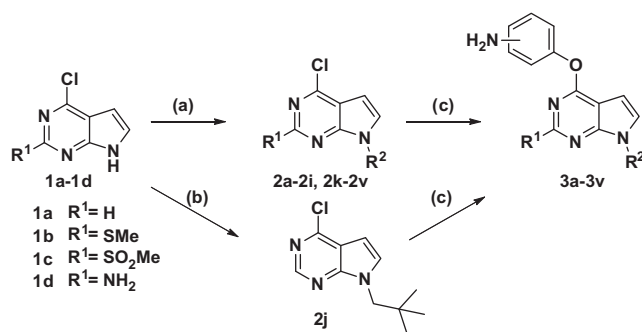
acids, quinolines, benzothiazoles, and other unique compounds such as naphthoquinone.^{4,5,13,22–24} Most of these classes of small molecules are competitive or noncompetitive inhibitors with respect to the substrates.⁴ In this paper, we describe luciferase inhibition by the substituted pyrrolo[2,3-*d*]pyrimidines that are structurally unrelated to these previously identified inhibitor classes with a novel unique mechanism of action.

The pyrrolo[2,3-*d*]pyrimidine scaffold is considered a privileged structure,²⁵ and it is frequently found in numerous biologically active molecules, including protein kinase inhibitors, microtubule targeting agents, and neurogenesis inducing molecules.²⁶ We found that the pyrrolo[2,3-*d*]pyrimidine compound **3a** (Fig. 1) is a novel potent firefly luciferase inhibitor, which emerged from a cell-based LPS/TLR4/NF- κ B signaling inhibitor screening. The pyrrolo[2,3-*d*]pyrimidine compound **3a** acts as a mixed-type, predominantly competitive inhibitor with respect to *D*-luciferin but an uncompetitive inhibitor with respect to ATP. A series of pyrrolo[2,3-*d*]pyrimidine analogues (**3b–3v**, **4a–4f**) were prepared to further explore their structure–activity relationships (SAR). We identified the compound **4c** as the most potent luciferase inhibitor. In addition, **3a** and **4c** (Fig. 1) were also docked at the *D*-luciferin binding site but not the ATP binding site of the crystal structure, which is suggestive of their partially competitive manner.

2. Results and discussion

2.1. Chemistry

The general method used for the synthesis of pyrrolo[2,3-*d*]pyrimidine derivatives is depicted in Schemes 2 and 3. The 4-chloro-7H-pyrrolo[2,3-*d*]pyrimidines **1** employed in these routes are commercially available. Substances **3a–3i**, **3k–3v** were prepared from compound **1** by an alkylation reaction with various alkyl halides and then a substitution with amino-phenol. In a similar manner, substance **3j** was obtained from compound **1** by Mitsunobu reaction with 2-dimethylpropan-1-ol, followed by the substitution reaction with amino-phenol. Substances **4a–4f** were generated from the corresponding substituted pyrrolo[2,3-*d*]pyrimidine via a methylation reaction.



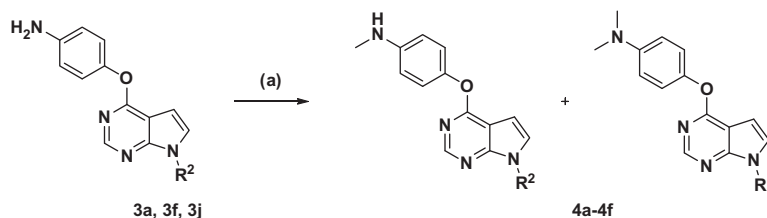
Scheme 2. Synthetic routes to the compounds. Reagents and conditions: (a) Alkyl halides, K_2CO_3 , DMF, 60–70 °C, 4–5 h; (b) 2,2-dimethylpropan-1-ol, THF, DEAD, $P(Ph)_3$, 0 °C –rt, overnight; (c) Amino-phenol, Cs_2CO_3 , DMSO, 80 °C, 6 h.

2.2. Structure–activity relationships

The inhibition of NF- κ B activation is now widely recognized as a valid drug-targeting strategy to combat inflammatory diseases. In an initial cell-based screen, our compound library was tested for activity on LPS/TLR4/NF- κ B signaling using the firefly luciferase reporter gene system.²⁷ This yielded a hit compound **3a** as an ‘active’ NF- κ B signaling inhibitor. **3a** still showed the inhibitory activity when further assessed with cells stably expressing firefly luciferase (after excluding the possibility of cytotoxicity). However, no immunosuppressive activities were found when monocytes were applied to study, which a NF- κ B signaling inhibitor should not display. We wondered whether compound **3a** is luciferase inhibitor rather than the NF- κ B signaling inhibitor, which might result in false positive hit. Therefore, we examined the ‘active’ compound **3a** in an in vitro enzymatic luciferase assay as described in Section 4. This led to discovering that compound **3a** displays significant enzymatic inhibition with an IC_{50} value of $0.36 \pm 0.05 \mu M$ (Fig. 2).

Because the luciferase assay is based on the readout of photon emission at 500–700 nm with a peak at 562 nm, nonspecific inhibition could arise through compound-specific absorbance or light scattering in this wavelength range. In this case, compounds that interfere with luminescence detection could appear as false-positive luciferase inhibitors. The absorbance spectrum (200–800 nm) was determined for compound **3a**, and the result showed that compound **3a** did not show any absorption at a wavelength higher than 300 nm (data not shown), which eliminated **3a** as the possible quencher of the luciferase signal.

Further studies were performed to investigate the kinetic characteristics of inhibition by **3a** because compound **3a** exerted a significant inhibitory activity on firefly luciferase. *D*-Luciferin was titrated in the absence and presence of three concentrations of **3a** (Fig. 3a), while holding the concentration of ATP constant at 250 μM . Re-plotting these data as a double reciprocal plot



Scheme 3. Synthetic route to the compounds **4a–4f**. Reagents and conditions: (a) MeI, NaH, DMF, rt, 6–7 h.

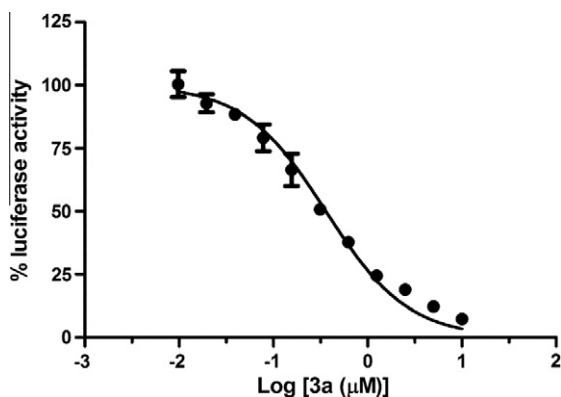


Figure 2. Inhibition of luciferase activity by compound **3a**. The IC_{50} value of **3a** was $0.36 \pm 0.05 \mu\text{M}$. Representative graph is from one of three independent experiments performed in triplicate.

generated a series of straight lines that crossed to the left of the $1/V$ axis and above the $1/[D\text{-luciferin}]$ axis (Fig. 3b). This is a typical form of mixed-type inhibition known as predominantly competitive inhibition. This suggests that **3a** can bind both to the free enzyme competing with D -luciferin for the active site and to the enzyme-luciferin complex, but with different affinities. Nonlinear regression analysis of the data with the Michaelis–Menten model showed that the presence of **3a** resulted in an increased apparent Michaelis constant (K_m^{app}) and a decreased apparent maximum velocity (V_{max}^{app}) in a dose dependent manner (Table 1). This result

was expected for a mixed-type inhibitor. Further nonlinear regression analysis of the data with a mixed-type inhibition model gave the dissociation constant (K_i) value of $0.22 \pm 0.05 \mu\text{M}$ and αK_i value of $1.43 \pm 0.92 \mu\text{M}$ (Table 1). Moreover, the K_m and V_{max} values of luciferase towards D -luciferin were $12 \pm 1 \mu\text{M}$ and $1.11 \pm 0.03 \times 10^5 \text{ RLU/ms}$, consistent with the values obtained from the analysis of the data in the absence of **3a** with Michaelis–Menten model, further proof of the rightness of the mixed-type inhibition model (Table 1).

Because luciferase has a second catalytic site for the other substrate ATP, a similar analysis was carried out to determine the type of inhibition with respect to ATP. D -Luciferin was held constant at $50 \mu\text{M}$, while ATP was titrated in the absence and presence of three concentrations of compound **3a** (Fig. 3c). A Lineweaver–Burk plot is quite different from the one obtained with D -luciferin, which showed a series of clearly parallel straight lines (Fig. 3d). This indicated that **3a** is uncompetitive with respect to ATP, which implies that **3a** targets the luciferase–ATP complex rather than free enzyme. As stated above, a nonlinear regression analysis of the data with Michaelis–Menten model was performed. The result indicated that the presence of **3a** resulted in a significant decrease in both K_m^{app} and V_{max}^{app} values in a dose dependent manner (Table 1), which is expected for an uncompetitive inhibitor. Further nonlinear regression analysis of the data directly with an uncompetitive inhibition model showed that the dissociation constant αK_i value of **3a** was $0.34 \pm 0.03 \mu\text{M}$, while the K_m and V_{max} values of luciferase with respect to ATP was $59 \pm 6 \mu\text{M}$ and $1.82 \pm 0.06 \times 10^5 \text{ RLU/ms}$. This result is consistent with the values obtained from the analysis of the data in the absence of **3a** with the Michaelis–Menten model,

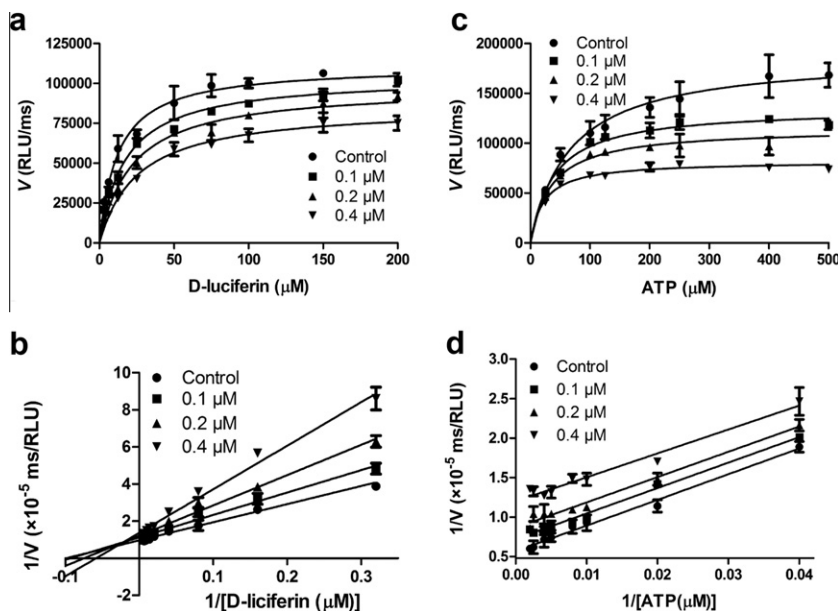


Figure 3. Kinetics of inhibition of luciferase by **3a**. The dependence of the initial velocity on the concentration of D -luciferin (a) or ATP (c) in the absence (Control) or presence of 0.1, 0.2 or 0.4 μM **3a**. The lines represent a nonlinear least squares fit of the Michaelis–Menten model to the data. The fit parameters, K_m^{app} and V_{max}^{app} are represented on Table 1. (b) A Lineweaver–Burk plot of data in (a). (d) A Lineweaver–Burk plot of data in (c). Representative graphs are from one experiment performed in triplicate.

Table 1
Kinetic parameters for the inhibition of luciferase by **3a** with respect to D-luciferin and ATP^a

	D-Luciferin ^b		ATP ^c	
	$K_m^{app}/\mu\text{M}$	$V_{max}^{app}/\times 10^5 \text{RLU ms}^{-1}$	$K_m^{app}/(\mu\text{M})$	$V_{max}^{app}/(\times 10^5 \text{RLU ms}^{-1})$
Control	12 ± 2	1.11 ± 0.04	67 ± 15	1.88 ± 0.12
0.1 μM 3a	17 ± 2	1.04 ± 0.03	39 ± 5	1.35 ± 0.04
0.2 μM 3a	22 ± 3	0.98 ± 0.04	35 ± 5	1.15 ± 0.04
0.4 μM 3a	26 ± 3	0.86 ± 0.03	22 ± 3	0.82 ± 0.02
$K_i/\mu\text{M}$	0.22 ± 0.05			
α	6.5 ± 2.7			
$\alpha K_i/\mu\text{M}$	1.43 ± 0.92		0.34 ± 0.03	
$V_{max}/\times 10^5 \text{RLU ms}^{-1}$	1.11 ± 0.03		1.82 ± 0.06	
$K_m/\mu\text{M}$	12 ± 1		59 ± 6	

^a Values are the means ± SEM of three independent assays performed in triplicate.

^b The dependence of luciferase activity on the concentration of luciferin at 250 μM ATP was assayed in the absence (Control) or presence of 0.1, 0.2 or 0.4 μM **3a**.

^c The dependence of luciferase activity on the concentration of ATP at 50 μM D-luciferin was determined in the absence (Control) or presence of 0.1, 0.2, or 0.4 μM **3a**, respectively.

which is further proof of the suitability of the uncompetitive inhibition model (Table 1). Additionally, Table 1 shows that the obtained K_m values of luciferase for D-luciferin (12 ± 1 μM) and ATP (59 ± 6 μM) were in good agreement with that reported by Lambert et al.²⁸ with a reaction system where albumin was used as an enzyme stabilization agent (8 ± 1 μM and 48 ± 2 μM, respectively).

Hence, **3a** appears to be predominantly competitive with respect to D-luciferin and uncompetitive with respect to ATP. These results suggest a model in which the initial steps generating a luciferase-ATP complex that can predominantly bind either **3a** or D-luciferin. Furthermore, the luciferase-ATP-D-luciferin complex can also bind **3a** at an allosteric site different from the substrate binding sites. Many inhibitors have been reported to inhibit the bioluminescent luciferase catalyzed reaction via specific or allosteric mechanisms. For example, oxyluciferin (a luciferin related substance) is a typical inhibitor with a specific inhibition mechanism,²¹ while anesthetics are typical examples of allosteric inhibitors.⁴ Compound **3a** differs from the inhibitors discussed above because it can bind both specific and allosteric sites in luciferase.

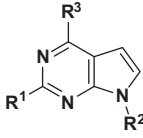
Table 2
Inhibition of luciferase activity by compounds **3a–3v**, expressed as IC₅₀ values or as% inhibition at 10 μM

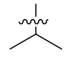
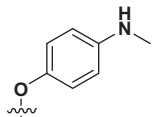
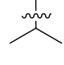
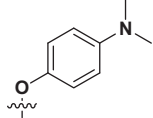
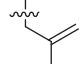
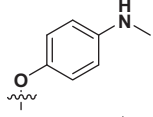
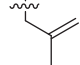
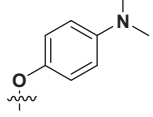
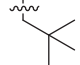
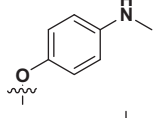
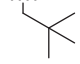
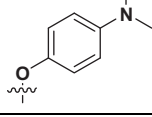
Compound	R ¹	R ²	R ³	IC ₅₀ (μM) or % inh. ^a	Compound	R ¹	R ²	R ³	IC ₅₀ (μM) or % inh. ^a
3a	H			0.36 ± 0.05	3l	H			7.53 ± 0.64
3b	H	H		19%	3m	H			21%
3c	H			48%	3n	H			33%
3d	H			3.51 ± 1.10	3o	H			46%
3e	H			0.31 ± 0.10	3p	H			26%
3f	H			0.12 ± 0.02	3q	H			7%
3g	H			9.43 ± 2.23	3r	H			14.71 ± 3.51
3h	H			0.29 ± 0.05	3s	H			7.30 ± 1.18
3i	H			2.24 ± 0.91	3t				31%
3j	H			0.08 ± 0.01	3u				9%
3k	H			6.46 ± 0.67	3v	NH ₂			10.76 ± 3.01

^a Inhibition of luciferase activity (IC₅₀ ± SEM (μM), n = 3, triplicate) or% inhibition at 10 μM (n = 3, triplicate).

Table 3

Inhibition of luciferase activity by compounds **4a–4f**, expressed as IC₅₀ values or as% inhibition at 10 μM



Compound	R ¹	R ²	R ³	IC ₅₀ (μM) ^a
4a	H			0.13 ± 0.03
4b	H			0.18 ± 0.05
4c	H			0.06 ± 0.01
4d	H			0.09 ± 0.0
4e	H			0.07 ± 0.02
4f	H			0.12 ± 0.04

^a Inhibition of luciferase activity (IC₅₀ ± SEM (μM), n = 3, triplicate) or% inhibition at 10 μM (n = 3, triplicate).

Many inhibitors are reported to be competitive or non-competitive inhibitors except for *l*-luciferin which acts as a mixed-type non-competitive-uncompetitive inhibitor¹⁹ towards *D*-luciferin, and naphthoquinone which is competitive with respect to *D*-luciferin and uncompetitive towards ATP.⁵ In our study, **3a** is a luciferase inhibitor with a new inhibition mechanism.

Subsequently, analogues of pyrrolo[2,3-*d*]pyrimidine that contain the 4-aminophenol group at the R₃ position were designed and tested for luciferase inhibition to explore the structure–activity relationships of this series of compounds (Table 2). Initially, substitutions at the R₂ position were investigated firstly, and it was noted that the activity was completely lost when R₂ was a hydrogen or methyl group (**3b**, **3c**). When R₂ was changed to an ethyl group, which has two carbons in length, compound **3d** displayed an inhibitory activity with an IC₅₀ value of 3.51 ± 1.10 μM, which was less potent than compound **3a**. We noted that the inhibitory activity could be improved by increasing the length of the substituents at the R₂ position. Next, the length and the steric effects of the substituents at the R₂ position were tested. Interestingly, we found that the substituents which contained bulky groups with three carbons in length (**3e**, **3f**, **3h**, **3j**) led to more potent activity. Among them, compound **3j** is the best, displaying an inhibitory activity with an IC₅₀ value of 0.08 ± 0.01 μM. The substituents that are less steric groups with three carbons in length (**3g**, **3i**) decreased the inhibitory activity. When the length of the

substituents were increased to four carbons (**3k**, **3l**), the inhibitory activity started to decrease. The introductions of heteroatoms at the R₂ substituents (**3m**, **3n**) were also detrimental to the activity. The substituents which contained aryl groups with or without the substituent (**3o**, **3p**, **3q**) led to the complete loss of activity. Secondly, an amino group at the *meta* or *ortho*-position of the phenol group at the R₃ position (**3r**, **3s**) led to the decrease in activity, which indicated that the 4-aminophenol group at the R₃ position is crucial for inhibitory activity. The introductions of electron donating or electron withdrawing groups at the R₁ position (**3t**, **3u**, **3v**) also abolished the inhibitory activity.

Other analogues having substituents at the amino group of the phenol ring were also synthesized and tested to determine if the hydrogen of the amino group is crucial for the inhibitory activity (Table 3). Interestingly, the mono-methyl substitution of the amino group as found in **4a**, **4c** and **4e** resulted in the highly potent luciferase inhibitors. The most potent luciferase inhibitor **4c** had an IC₅₀ value of 0.06 ± 0.01 μM, whereas the di-methyl substitution of the amino group (**4b**, **4d**, **4f**) remained the potency (Table 3).

Finally, to investigate the molecular basis of these derivatives interacting with luciferase, a molecular docking approach was performed to analyze the complex structures of **3a** and **4c** with the enzyme. From the crystal structures of firefly luciferase with inhibitor and AMP, we know that there are two different binding pockets within the enzyme. The AMP binding pocket is curved while the flat one is for oxyluciferin.²⁹ As shown in Figure 4 (left), the best poses obtained (lowest predicted binding free energy of the most occurring binding mode) for both **3a** and **4c** are accommodated well by the oxyluciferin binding pocket, as expected for a predominantly competitive inhibitor with respect to *D*-luciferin. For **3a**, the amino group attached to the phenyl ring provided the hydrophobic interactions with the carbonyl group of Asn229 and carboxyl group of Glu311. The nitrogen atom on the pyrimidine formed a hydrogen bond with the hydroxyl of residue Ser347. Moreover, the pyrrole ring of **3a** provided an aromatic stacking with residue Phe247, which might play a major role in ligand binding (Fig. 4, top right). We also noticed that the oxyluciferin pocket was so flat and narrow that the substituent at the R₁ position was not tolerated. Thus compounds **3t**, **3u**, and **3v** showed little inhibitory activities. Interestingly, based on the conformation obtained of **4c**, we observed that the binding between luciferase and **4c** might be a result of the hydrophobic interactions and well-accommodated space in the pocket (Fig. 4, lower right). The binding modes of the two ligands suggested that hydrophobic residues, such as Phe247 of the enzyme, might play major roles in ligand binding. Thus, the analogues with hydrophilic groups near residue Phe247 showed low activities, such as **3m** and **3n**. In addition, the pocket space near residue Phe247 was so narrow that larger groups were not allowed, which might explain why the introduction of a phenyl ring (**3o**, **3p**, **3q**) was not favorable for inhibitory activity.

3. Conclusions

In summary, we have shown that ‘drug-like’ compounds, such as **3a** or **4c**, are mixed-type predominantly competitive inhibitors of firefly luciferase with respect to substrate *D*-luciferin. Meanwhile, these compounds are uncompetitive inhibitors with respect to ATP. The inclusion of these similar compounds would result in a high number of ‘hits’ in screening campaigns that rely on fire luciferase reporter-gene assays. When these ‘hits’ were further evaluated with other bioactivity assays, they could be found to be ‘false negatives’ or ‘false positives’. Notably, pyrrolo[2,3-*d*]pyrimidine frameworks are ubiquitous structures in a wide variety of naturally occurring and synthetic compounds that exhibit important biological activity, such as a variety of kinase inhibitors^{30,31} and antivirals.^{32,33} Thus, they are widely used in the screening of compound

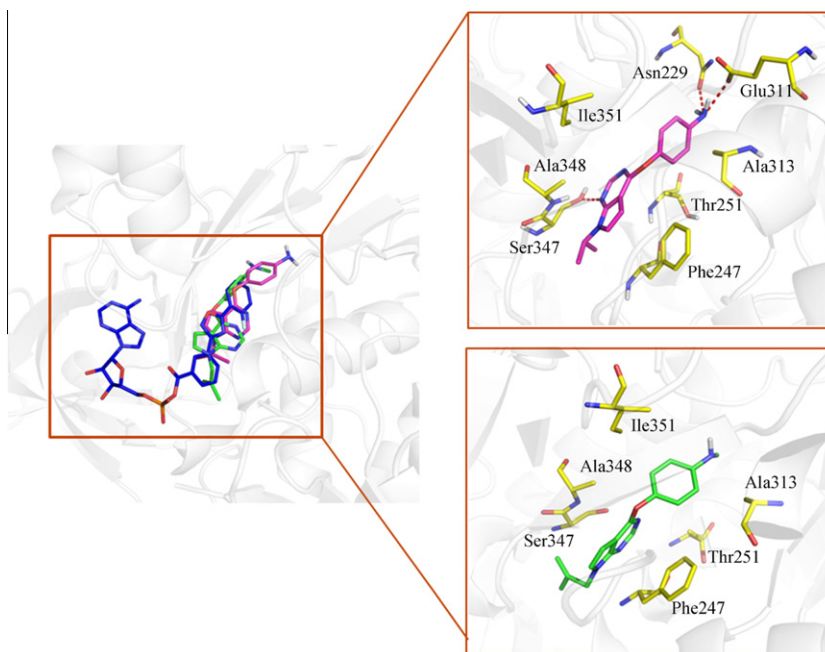


Figure 4. Predicted conformations of **3a** and **4c** in the binding pocket of luciferase. **3a** is shown in magenta sticks. **4c** is shown in green sticks, and PTC124-AMP (conformation provided by the crystal structure 3IES) is shown in blue sticks. Residues in the binding pocket forming hydrophobic or hydrogen-bond interactions with compounds are indicated in yellow sticks on the right.

libraries. Hence, the compounds that we found in this paper were ‘flagged’ as firefly luciferase inhibitors, and they could be added into a counter screen database to exclude the interferences of HTS in which a luciferase reporter system was increasingly used.^{11,13} Additionally, all the novel luciferase inhibitors with a unique mechanism of action described here should be useful to the scientific community for investigating the mechanism of luciferase catalyzed reactions and better understanding the activity of the other oxygenases.

4. Experimental section

4.1. Chemistry: material and methods

All reagents used were obtained from commercial sources, and all solvents were of analytical grade. ¹H NMR spectral data were recorded in DMSO-*d*₆, CD₃OD or CDCl₃ on Varian Mercury 400 or 300 NMR spectrometer and ¹³C NMR were recorded in DMSO-*d*₆ or CDCl₃ on Varian Mercury 100 NMR spectrometer. Chemical shifts (δ) were reported in parts per million (ppm), and the signals were described as brs (broad singlet), d (doublet), dd (doublet of doublet), m (multiple), q (quarter), s (singlet), and t (triplet). Coupling constants (*J* values) were given in Hz. Low-resolution mass spectra (MS) and high-resolution mass spectra (HRMS) were recorded at an ionizing voltage of 70 eV on a Finnigan/MAT95 spectrometer. Column chromatography was carried out on silica gel (200–300 mesh). All reactions were monitored using thin-layer chromatography (TLC) on silica gel plates. Yields were of purified compounds and were not optimized.

4.1.1. General procedure for the synthesis of **3a**, **3e–3i** and **3k–3v** from **1**

A typical procedure for the preparation of **3a**: 2-bromopropane (74 mg, 0.6 mmol) was added to a solution of **1a** (92 mg, 0.6 mmol) and K₂CO₃ (110 mg, 0.8 mmol) in 5 mL DMF at 70 °C. According to TLC the reaction went to completion after 4 h. The mixture was extracted with ethyl acetate (3 × 10 mL). The combined organic layers were washed with brine (10 mL), dried over anhydrous Na₂SO₄, filtered and concentrated to give the crude product **2a**, which was

added to a solution of amino-phenol (66 mg, 0.6 mmol) and Cs₂CO₃ (585 mg, 1.8 mmol) in 10 mL DMSO without further purification. After stirring for 6 h at 80 °C, the mixture was cooled to room temperature and extracted with ethyl acetate (3 × 10 mL). The combined organic layers were washed with brine (10 mL), dried over anhydrous Na₂SO₄, filtered and concentrated to give the crude product, which was further purified by column chromatography (petroleum ether/ethyl acetate 2:1) to afford compound **3a** as a brown solid (121 mg, 75% over two steps): ¹H NMR (300 MHz, CDCl₃) δ 8.44 (s, 1H), 7.16 (d, *J* = 3.6 Hz, 1H), 7.02 (d, *J* = 8.9 Hz, 2H), 6.73 (d, *J* = 8.9 Hz, 2H), 6.39 (d, *J* = 3.6 Hz, 1H), 5.11 (m, 1H), 3.70 (s, 2H), 1.51 (d, *J* = 6.8 Hz, 6H).; ¹³C NMR (100 MHz, *d*₆-DMSO) δ 162.5, 151.5, 150.0, 146.3, 142.7, 124.5, 122.2, 114.3, 104.6, 98.0, 46.0, 22.3.; HRMS [M]⁺ calcd for C₁₅H₁₆N₄O 268.1324, found 268.1326. The purity of the compound was >98% by HPLC.

4.1.2. 4-(4-Aminophenoxy)-7H-pyrrolo[2,3-d]pyrimidine (**3b**)

Compound **1a** (92 mg, 0.6 mmol) was added to a solution of amino-phenol (66 mg, 0.6 mmol) and Cs₂CO₃ (585 mg, 1.8 mmol) in 10 mL DMSO. After stirring for 9 h at 80 °C, the mixture was cooled to room temperature and extracted with ethyl acetate (3 × 10 mL). The combined organic layers were washed with brine (10 mL), dried over anhydrous Na₂SO₄, filtered and concentrated to give the crude product, which was further purified by column chromatography (petroleum ether/ethyl acetate 2:1) to afford compound **3b** as a brown solid (92 mg, 68%): ¹H NMR (300 MHz, *d*₆-DMSO) δ 12.12 (s, 1H), 8.27 (s, 1H), 7.38 (d, *J* = 3.0 Hz, 1H), 6.89 (d, *J* = 8.7 Hz, 2H), 6.60 (d, *J* = 8.7 Hz, 2H), 6.24 (d, *J* = 3.1 Hz, 1H), 5.06 (s, 2H).; ¹³C NMR (100 MHz, *d*₆-DMSO) δ 162.5, 153.4, 150.3, 146.3, 142.8, 124.6, 122.2, 114.3, 104.3, 98.2.; HRMS [M]⁺ calcd for C₁₂H₁₀N₄O 226.0855, found 226.0854. The purity of the compound was >95% by HPLC.

4.1.3. 7-Methyl-4-(4-aminophenoxy)-7H-pyrrolo[2,3-d]pyrimidine (**3c**)

Iodomethane (0.04 ml, 0.6 mmol) was added to a solution of **1a** (92 mg, 0.6 mmol), NaH (24 mg 60%, 0.6 mmol) in 5 mL dry THF at 0 °C. After stirring for 3 h at room temperature, the reaction went

to completion according to TLC. Water (10 mL) was added and the mixture was extracted with ethyl acetate (3 × 10 mL). The combined organic layers were washed with brine (10 mL), dried over anhydrous Na₂SO₄, filtered and concentrated to give the crude product, which was added to a solution of amino-phenol (66 mg, 0.6 mmol) and Cs₂CO₃ (585 mg, 1.8 mmol) in 10 mL DMSO without further purification. After stirring for 6 h at 80 °C, the mixture was cooled to room temperature and extracted with ethyl acetate (3 × 10 mL). The combined organic layers were washed with brine (10 mL), dried over anhydrous Na₂SO₄, filtered and concentrated to give the crude product, which was further purified by column chromatography (petroleum ether/ethyl acetate 2:1) to afford compound **3c** as a yellow solid (104 mg, 72% over two steps): ¹H NMR (300 MHz, CDCl₃) δ 8.40 (s, 1H), 7.02–6.91 (m, 3H), 6.67 (d, *J* = 8.6 Hz, 2H), 6.31 (d, *J* = 3.5 Hz, 1H), 3.80 (s, 3H), 2.82 (s, 2H); ¹³C NMR (100 MHz, *d*₆-DMSO) δ 162.4, 152.3, 150.2, 146.1, 142.8, 128.7, 122.2, 114.4, 104.4, 97.6, 31.1; HRMS [M]⁺ calcd for C₁₃H₁₂N₄O 240.1011, found 240.1009. The purity of the compound was >98% by HPLC.

4.1.4. 7-Ethyl-4-(4-aminophenoxy)-7H-pyrrolo[2,3-d]pyrimidine (3d)

Iodoethane (0.05 ml, 0.6 mmol) was added to a solution of **1a** (92 mg, 0.6 mmol), NaH (24 mg 60%, 0.6 mmol) in 5 mL dry THF at 0 °C. After stirring for 3 h at room temperature, the reaction went to completion according to TLC. Water (10 mL) was added and the mixture was extracted with ethyl acetate (3 × 10 mL). The combined organic layers were washed with brine (10 mL), dried over anhydrous Na₂SO₄, filtered and concentrated to give the crude product, which was added to a solution of amino-phenol (66 mg, 0.6 mmol) and Cs₂CO₃ (585 mg, 1.8 mmol) in 10 mL DMSO without further purification. After stirring for 6 h at 80 °C, the mixture was cooled to room temperature and extracted with ethyl acetate (3 × 10 mL). The combined organic layers were washed with brine (10 mL), dried over anhydrous Na₂SO₄, filtered and concentrated to give the crude product, which was further purified by column chromatography (petroleum ether/ethyl acetate 2:1) to afford compound **3d** as a yellow solid (93 mg, 61% over two steps): ¹H NMR (300 MHz, CDCl₃) δ 8.46 (s, 1H), 7.09 (d, *J* = 3.5 Hz, 1H), 7.03 (d, *J* = 8.7 Hz, 2H), 6.74 (d, *J* = 8.7 Hz, 2H), 6.38 (d, *J* = 3.5 Hz, 1H), 4.30 (q, *J* = 7.3 Hz, 2H), 3.68 (s, 2H), 1.47 (t, *J* = 7.3 Hz, 3H); ¹³C NMR (100 MHz, *d*₆-DMSO) δ 162.5, 151.8, 150.1, 146.3, 142.7, 127.2, 122.24, 114.3, 104.5, 97.8, 39.2, 15.4; HRMS [M]⁺ calcd for C₁₄H₁₄N₄O 254.1168, found 254.1171. The purity of the compound was >97% by HPLC.

4.1.5. 7-Isobutyl-4-(4-aminophenoxy)-7H-pyrrolo[2,3-d]pyrimidine (3e)

Brown solid (69%); ¹H NMR (300 MHz, CDCl₃) δ 8.45 (s, 1H), 7.03 (dd, *J* = 6.1, 4.2 Hz, 3H), 6.73 (d, *J* = 8.9 Hz, 2H), 6.39 (d, *J* = 3.5 Hz, 1H), 4.04 (d, *J* = 7.4 Hz, 2H), 3.68 (s, 2H), 2.29–2.14 (m, 1H), 0.92 (d, *J* = 6.7 Hz, 6H); ¹³C NMR (100 MHz, *d*₆-DMSO) δ 154.1, 153.1, 150.8, 149.7, 131.5, 125.1, 123.2, 114.9, 103.0, 98.1, 51.0, 29.0, 19.7; HRMS [M]⁺ calcd for C₁₆H₁₈N₄O 282.1481, found 282.1485. The purity of the compound was >95% by HPLC.

4.1.6. 7-(2-Methylallyl)-4-(4-aminophenoxy)-7H-pyrrolo[2,3-d]pyrimidine (3f)

Yellow solid (76%); ¹H NMR (300 MHz, CDCl₃) δ 8.31 (s, 1H), 7.28 (d, *J* = 3.6 Hz, 1H), 6.97 (d, *J* = 8.8 Hz, 2H), 6.74 (d, *J* = 8.8 Hz, 2H), 6.40 (d, *J* = 3.6 Hz, 1H), 4.86 (m, 3H), 4.66 (m, 3H), 1.67 (s, 3H); ¹³C NMR (100 MHz, *d*₆-DMSO) δ 162.6, 152.3, 150.4, 146.4, 142.7, 141.5, 127.9, 122.2, 114.3, 111.8, 104.4, 98.1, 49.5, 19.8; HRMS [M]⁺ calcd for C₁₆H₁₆N₄O 280.1324, found 280.1330. The purity of the compound was >98% by HPLC.

4.1.7. 7-(Propa-1,2-dien-1-yl)-4-(4-aminophenoxy)-7H-pyrrolo[2,3-d]pyrimidine (3g)

Off white solid (70%); ¹H NMR (300 MHz, CD₃OD) δ 8.33 (s, 1H), 7.63 (t, *J* = 6.5 Hz, 1H), 7.34 (d, *J* = 3.7 Hz, 1H), 6.96 (d, *J* = 7.6 Hz, 2H), 6.79 (d, *J* = 8.5 Hz, 2H), 6.25 (d, *J* = 3.6 Hz, 1H), 5.70 (d, *J* = 7.4 Hz, 3H); ¹³C NMR (100 MHz, *d*₆-DMSO) δ 201.6, 162.7, 151.3, 151.1, 146.5, 142.5, 124.3, 122.1, 114.3, 105.3, 100.6, 94.5, 89.1; HRMS [M]⁺ calcd for C₁₅H₁₂N₄O 264.1011, found 264.1016. The purity of the compound was >97% by HPLC.

4.1.8. 7-Cyclopentyl-4-(4-aminophenoxy)-7H-pyrrolo[2,3-d]pyrimidine (3h)

Off white solid (77%); ¹H NMR (300 MHz, CDCl₃) δ 8.45 (s, 1H), 7.15 (d, *J* = 3.6 Hz, 1H), 7.02 (d, *J* = 8.7 Hz, 2H), 6.74 (d, *J* = 8.7 Hz, 2H), 6.39 (d, *J* = 3.6 Hz, 1H), 5.30–5.10 (m, 1H), 3.67 (s, 2H), 2.31–2.14 (m, 2H), 1.95–1.74 (m, 6H); ¹³C NMR (100 MHz, *d*₆-DMSO) δ 162.5, 152.1, 150.0, 146.4, 142.8, 125.2, 122.2, 114.3, 104.7, 98.1, 55.3, 32.2, 23.6; HRMS [M]⁺ calcd for C₁₇H₁₈N₄O 294.1481, found 294.1479. The purity of the compound was >95% by HPLC.

4.1.9. 7-Allyl-4-(4-aminophenoxy)-7H-pyrrolo[2,3-d]pyrimidine (3i)

Off white solid (64%); ¹H NMR (300 MHz, CDCl₃) δ 8.46 (s, 1H), 7.06 (d, *J* = 3.5 Hz, 1H), 7.03 (d, *J* = 8.9 Hz, 2H), 6.73 (d, *J* = 8.9 Hz, 2H), 6.42 (d, *J* = 3.5 Hz, 1H), 6.01 (m, 1H), 5.23 (d, *J* = 10.2 Hz, 1H), 5.11 (d, *J* = 17.1 Hz, 1H), 4.87 (d, *J* = 5.5 Hz, 2H), 3.68 (s, 2H); ¹³C NMR (100 MHz, *d*₆-DMSO) δ 154.1, 153.2, 151.0, 149.4, 134.3, 131.4, 124.5, 123.2, 116.7, 115.0, 103.0, 98.7, 45.9; HRMS [M]⁺ calcd for C₁₅H₁₄N₄O 266.1168, found 266.1170. The purity of the compound was >95% by HPLC.

4.1.10. 7-Neopentyl-4-(4-aminophenoxy)-7H-pyrrolo[2,3-d]pyrimidine (3j)

Diethyl azodicarboxylate (140 mg, 0.8 mmol) was added to a solution of **1a** (92 mg, 0.6 mmol), 2, 2-dimethylpropan-1-ol (53 mg, 0.6 mmol) and triphenylphosphine (160 mg, 0.6 mmol), in 10 mL THF at 0 °C under nitrogen atmosphere. After stirring for 6 h at room temperature, the reaction went to completion according to TLC. The mixture was extracted with ethyl acetate (3 × 10 mL). The combined organic layers were washed with brine (10 mL), dried over anhydrous Na₂SO₄, filtered and concentrated to give the crude product, which was further purified by column chromatography (petroleum ether/ethyl acetate 4:1) to afford compound **2j**. Compound **2j** was added to a solution of amino-phenol (66 mg, 0.6 mmol) and Cs₂CO₃ (585 mg, 1.8 mmol) in 10 mL DMSO at 80 °C. After stirring for 6 h, the mixture was cooled to room temperature and extracted with ethyl acetate (3 × 10 mL). The combined organic layers were washed with brine (10 mL), dried over anhydrous Na₂SO₄, filtered and concentrated to give the crude product, which was further purified by column chromatography (petroleum ether/ethyl acetate 2:1) to afford compound **3j** as a white solid (98 mg, 55% over two steps): ¹H NMR (300 MHz, CDCl₃) δ 8.44 (s, 1H), 7.04 (d, *J* = 3.5 Hz, 1H), 7.02 (d, *J* = 8.7 Hz, 2H), 6.71 (d, *J* = 8.6 Hz, 2H), 6.40 (s, 1H), 4.04 (s, 2H), 3.68 (s, 2H), 0.97 (s, 9H); ¹³C NMR (100 MHz, *d*₆-DMSO) δ 162.9, 153.2, 150.6, 144.8, 143.9, 127.8, 122.4, 115.8, 104.9, 97.9, 55.9, 33.6, 27.7; HRMS [M]⁺ calcd for C₁₇H₂₀N₄O 296.1637, found 296.1636. The purity of the compound was >99% by HPLC.

4.1.11. 7-Cyclopentyl-4-(4-aminophenoxy)-7H-pyrrolo[2,3-d]pyrimidine (3k)

Brown solid (62%); ¹H NMR (300 MHz, CDCl₃) δ 8.30 (s, 1H), 7.36 (d, *J* = 3.5 Hz, 1H), 6.96 (d, *J* = 8.8 Hz, 2H), 6.74 (d, *J* = 8.8 Hz, 2H), 6.35 (d, *J* = 3.5 Hz, 1H), 4.67 (s, 2H), 4.31 (s, 2H), 1.74 (q, *J* = 7.5 Hz, 2H), 1.51 (m, 1H), 0.94 (d, *J* = 6.6 Hz, 6H); ¹³C NMR

(100 MHz, d_6 -DMSO) δ 162.5, 152.0, 150.1, 146.3, 142.7, 127.6, 122.2, 114.2, 104.4, 97.8, 42.4, 38.5, 25.1, 22.2.; HRMS [M]⁺ calcd for C₁₇H₂₀N₄O 296.1637, found 296.1634. The purity of the compound was >99% by HPLC.

4.1.12. 7-Allyl-4-(4-aminophenoxy)-7H-pyrrolo[2,3-d]pyrimidine (3l)

Off white solid (58%); ¹H NMR (300 MHz, CDCl₃) δ 8.46 (s, 1H), 7.06 (d, J = 3.6 Hz, 1H), 7.03 (d, J = 8.7 Hz, 2H), 6.74 (d, J = 8.7 Hz, 2H), 6.38 (d, J = 3.5 Hz, 1H), 5.41 (t, J = 7.5 Hz, 1H), 4.83 (d, J = 7.1 Hz, 2H), 3.67 (s, 2H), 1.82 (s, 3H), 1.78 (s, 3H).; ¹³C NMR (100 MHz, d_6 -DMSO) δ 162.5, 151.8, 150.2, 146.3, 142.7, 136.3, 127.2, 122.1, 119.7, 114.2, 104.4, 97.9, 41.8, 25.3, 17.8.; HRMS [M]⁺ calcd for C₁₇H₁₈N₄O 294.1481, found 294.1482. The purity of the compound was >95% by HPLC.

4.1.13. 2-(4-(4-Aminophenoxy)-7H-pyrrolo[2,3-d]pyrimidin-7-yl)acetamide (3m)

Off white solid (56%); ¹H NMR (300 MHz, CDCl₃) δ 8.29 (s, 1H), 7.65 (s, 1H), 7.40 (d, J = 3.3 Hz, 1H), 7.25 (s, 1H), 6.89 (d, J = 8.6 Hz, 2H), 6.61 (d, J = 8.6 Hz, 2H), 6.24 (d, J = 3.3 Hz, 1H), 5.07 (s, 2H), 4.87 (s, 2H).; ¹³C NMR (100 MHz, d_6 -DMSO) δ 168.9, 162.5, 152.6, 150.2, 146.4, 142.7, 129.2, 122.2, 114.3, 104.5, 97.6, 46.5.; HRMS [M]⁺ calcd for C₁₄H₁₃N₅O₂ 283.1069, found 283.1071. The purity of the compound was >96% by HPLC.

4.1.14. Ethyl 2-(4-(4-aminophenoxy)-7H-pyrrolo[2,3-d]pyrimidin-7-yl)acetate (3n)

Off white solid (53%); ¹H NMR (300 MHz, CDCl₃) δ 8.45 (s, 1H), 7.08 (d, J = 3.6 Hz, 1H), 7.02 (d, J = 8.7 Hz, 2H), 6.72 (d, J = 8.7 Hz, 2H), 6.45 (d, J = 3.6 Hz, 1H), 5.01 (s, 2H), 4.24 (q, J = 7.1 Hz, 2H), 3.69 (s, 2H), 1.28 (t, J = 7.1 Hz, 3H).; ¹³C NMR (100 MHz, d_6 -DMSO) δ 168.3, 162.5, 152.5, 150.5, 146.4, 142.6, 128.6, 122.2, 114.2, 104.4, 98.1, 61.1, 45.5, 14.0.; HRMS [M]⁺ calcd for C₁₆H₁₆N₄O₃ 312.1222, found 312.1223. The purity of the compound was >95% by HPLC.

4.1.15. 7-Benzyl-4-(4-aminophenoxy)-7H-pyrrolo[2,3-d]pyrimidine (3o)

Brown oil (71%); ¹H NMR (300 MHz, CDCl₃) δ 8.34 (s, 1H), 7.54 (d, J = 3.5 Hz, 1H), 7.33–7.29 (m, 2H), 7.25 (t, J = 7.1 Hz, 3H), 6.89 (d, J = 8.7 Hz, 2H), 6.61 (d, J = 8.7 Hz, 2H), 6.30 (d, J = 3.5 Hz, 1H), 5.45 (s, 2H), 5.08 (s, 2H).; ¹³C NMR (100 MHz, d_6 -DMSO) δ 162.6, 152.1, 150.5, 146.4, 142.6, 137.7, 128.6, 127.8, 127.5, 127.3, 122.2, 114.2, 104.5, 98.3, 47.5.; HRMS [M]⁺ calcd for C₁₉H₁₆N₄O 316.1324, found 316.1326. The purity of the compound was >98% by HPLC.

4.1.16. 7-(4-Methoxybenzyl)-4-(4-aminophenoxy)-7H-pyrrolo[2,3-d]pyrimidine (3p)

Off white solid (75%); ¹H NMR (300 MHz, d_6 -DMSO) δ 8.35 (s, 1H), 7.51 (d, J = 3.5 Hz, 1H), 7.24 (d, J = 8.6 Hz, 2H), 6.88 (t, J = 9.1 Hz, 4H), 6.61 (d, J = 8.7 Hz, 2H), 6.28 (d, J = 3.5 Hz, 1H), 5.36 (s, 2H), 5.08 (s, 2H), 3.70 (s, 3H).; ¹³C NMR (100 MHz, d_6 -DMSO) δ 163.0, 159.2, 152.6, 151.1, 144.9, 144.0, 128.9, 126.0, 122.5, 115.8, 114.1, 105.3, 99.0, 55.2, 47.6.; HRMS [M]⁺ calcd for C₂₀H₁₈N₄O₂ 346.1430, found 346.1426. The purity of the compound was >98% by HPLC.

4.1.17. 4-(4-Nitrophenoxy)-7-(4-(trifluoromethyl)benzyl)-7H-pyrrolo[2,3-d]pyrimidine (3q)

Brown solid (80%); ¹H NMR (300 MHz, CDCl₃) δ 8.48 (s, 1H), 7.58 (d, J = 8.1 Hz, 2H), 7.31 (d, J = 8.0 Hz, 2H), 7.08–7.01 (m, 3H), 6.75 (d, J = 8.5 Hz, 2H), 6.47 (d, J = 3.5 Hz, 1H), 5.51 (s, 2H), 3.70 (s, 2H).; ¹³C NMR (100 MHz, CDCl₃) δ 163.1, 152.7, 151.3, 144.8, 144.1, 140.8, 130.2, 129.9, 127.5, 126.0, 125.7, 122.4, 115.9,

105.4, 99.6, 47.7.; HRMS [M]⁺ calcd for C₂₀H₁₅F₃N₄O 314.1198, found 314.1195. The purity of the compound was >96% by HPLC.

4.1.18. 7-Isopropyl-4-(3-aminophenoxy)-7H-pyrrolo[2,3-d]pyrimidine (3r)

White solid (71%); ¹H NMR (300 MHz, CDCl₃) δ 8.47 (s, 1H), 7.20 (dd, J = 12.6, 5.2 Hz, 2H), 6.64–6.56 (m, 3H), 6.42 (d, J = 3.4 Hz, 1H), 5.12 (dt, J = 13.5, 6.8 Hz, 1H), 3.76 (s, 2H), 1.53 (d, J = 6.7 Hz, 6H).; ¹³C NMR (100 MHz, CDCl₃) δ 162.3, 154.0, 152.0, 150.5, 147.8, 130.1, 122.8, 112.3, 111.5, 108.4, 105.7, 98.6, 46.1, 22.7.; HRMS [M]⁺ calcd for C₁₅H₁₆N₄O 268.1324, found 268.1322. The purity of the compound was >99% by HPLC.

4.1.19. 7-Isopropyl-4-(2-aminophenoxy)-7H-pyrrolo[2,3-d]pyrimidine (3s)

Off white solid (66%); ¹H NMR (300 MHz, CDCl₃) δ 8.47 (s, 1H), 7.18 (d, J = 3.6 Hz, 1H), 7.12 (m, 2H), 6.88 (dd, J = 8.3, 1.5 Hz, 1H), 6.83 (td, J = 7.5, 1.5 Hz, 1H), 6.36 (d, J = 3.6 Hz, 1H), 5.12 (dt, J = 13.5, 6.7 Hz, 1H), 3.76 (s, 2H), 1.53 (d, J = 6.8 Hz, 6H).; ¹³C NMR (100 MHz, CDCl₃) δ 161.8, 152.1, 150.6, 140.1, 139.1, 126.5, 123.0, 122.6, 118.7, 116.8, 105.3, 98.4, 46.2, 22.7.; HRMS [M]⁺ calcd for C₁₅H₁₆N₄O 268.1324, found 268.1328. The purity of the compound was >98% by HPLC.

4.1.20. 7-Isopropyl-2-(methylthio)-4-(4-aminophenoxy)-7H-pyrrolo[2,3-d]pyrimidine (3t)

Off white solid (63%); ¹H NMR (300 MHz, CDCl₃) δ 7.02 (d, J = 8.8 Hz, 2H), 6.94 (d, J = 3.6 Hz, 1H), 6.69 (d, J = 8.6 Hz, 2H), 6.03 (d, J = 3.6 Hz, 1H), 5.03 (dt, J = 13.6, 6.8 Hz, 1H), 3.69 (s, 2H), 2.48 (s, 3H), 1.47 (d, J = 6.8 Hz, 6H).; ¹³C NMR (100 MHz, d_6 -DMSO) δ 162.0, 161.9, 152.4, 146.4, 142.6, 123.3, 122.1, 114.2, 101.4, 98.3, 46.1, 22.2, 13.6.; HRMS [M]⁺ calcd for C₁₆H₁₈N₄OS 314.1201, found 314.1202. The purity of the compound was >98% by HPLC.

4.1.21. 7-Allyl-4-(4-aminophenoxy)-7H-pyrrolo[2,3-d]pyrimidine (3u)

Off white solid (62%); ¹H NMR (300 MHz, CDCl₃) δ 7.33 (d, J = 3.6 Hz, 1H), 7.02 (d, J = 8.7 Hz, 2H), 6.72 (d, J = 8.8 Hz, 2H), 6.39 (d, J = 3.6 Hz, 1H), 5.23 (dt, J = 13.5, 6.8 Hz, 1H), 3.20 (s, 3H), 1.52 (d, J = 6.8 Hz, 6H).; ¹³C NMR (100 MHz, d_6 -DMSO) δ 162.5, 156.8, 150.3, 146.8, 142.3, 128.0, 121.9, 114.2, 106.0, 99.3, 46.8, 22.3.; HRMS [M]⁺ calcd for C₁₆H₁₈N₄O₃ 346.1100, found 346.1103. The purity of the compound was >95% by HPLC.

4.1.22. 7-Isopropyl-2-amino-4-(4-aminophenoxy)-7H-pyrrolo[2,3-d]pyrimidine (3v)

White solid (71%); ¹H NMR (300 MHz, CDCl₃) δ 7.01 (d, J = 8.8 Hz, 2H), 6.77 (d, J = 3.7 Hz, 1H), 6.70 (d, J = 8.8 Hz, 2H), 5.90 (d, J = 3.7 Hz, 1H), 4.88 (dt, J = 13.2, 6.5 Hz, 1H), 4.72 (s, 2H), 3.66 (s, 2H), 1.43 (d, J = 6.8 Hz, 6H).; ¹³C NMR (100 MHz, d_6 -DMSO) δ 168.3, 164.4, 159.3, 151.2, 148.2, 127.4, 124.6, 119.4, 103.5, 102.2, 49.9, 27.4.; HRMS [M]⁺ calcd for C₁₅H₁₇N₅O 283.1433, found 283.1430. The purity of the compound was >98% by HPLC.

4.1.23. General procedure for the synthesis of 4a–4f

A typical procedure for the preparation of **4e** and **4f**. Iodomethane (0.065 ml, 1.0 mmol) was added to a solution of **3j** (178 mg, 0.6 mmol), NaH (40 mg 60%, 1.0 mmol) in 10 mL dry THF at 0 °C. After stirring for 8 h at room temperature, the reaction went to completion according to TLC. Water (10 mL) was added and the mixture was extracted with ethyl acetate (3 × 10 mL). The combined organic layers were washed with brine (10 mL), dried over anhydrous Na₂SO₄, filtered and concentrated to give the crude product, which was further purified by column chromatography (petroleum ether/ethyl acetate 8:1) to afford compounds **4e** and **4f** (2:3). **4e** as a yellow oil (56 mg, 30%); ¹H NMR (300 MHz, CDCl₃)

δ 8.45 (s, 1H), 7.09–7.05 (m, 3H), 6.66 (d, J = 8.9 Hz, 2H), 6.40 (d, J = 3.5 Hz, 1H), 4.06 (s, 2H), 3.76 (s, 1H), 2.86 (s, 3H), 0.99 (s, 9H); ^{13}C NMR (100 MHz, CDCl_3) δ 163.1, 153.2, 150.8, 147.0, 144.0, 127.8, 122.4, 112.9, 104.9, 98.0, 56.0, 33.7, 31.0, 27.8; HRMS $[\text{M}]^+$ calcd for $\text{C}_{18}\text{H}_{22}\text{N}_4\text{O}$ 310.1794, found 310.1798. The purity of the compound was >99% by HPLC.; **4f** as a light green (88 mg, 45%): ^1H NMR (300 MHz, CDCl_3) δ 8.45 (s, 1H), 7.12 (d, J = 9.1 Hz, 2H), 7.05 (d, J = 3.5 Hz, 1H), 6.78 (d, J = 9.1 Hz, 2H), 6.41 (d, J = 3.5 Hz, 1H), 4.06 (s, 2H), 2.96 (s, 6H), 0.99 (s, 9H); ^{13}C NMR (100 MHz, CDCl_3) δ 163.1, 153.2, 150.8, 148.4, 143.6, 127.8, 122.1, 113.3, 104.9, 98.0, 56.0, 40.9, 33.7, 27.7; HRMS $[\text{M}]^+$ calcd for $\text{C}_{19}\text{H}_{24}\text{N}_4\text{O}$ 324.1950, found 324.1952. The purity of the compound was >98% by HPLC.

4.1.24. 7-Isopropyl-4-(4-methylaminophenoxy)-7H-pyrrolo[2,3-d]pyrimidine (4a)

Off white solid (27%); ^1H NMR (300 MHz, CDCl_3) δ 8.45 (s, 1H), 7.16 (d, J = 3.6 Hz, 1H), 7.06 (d, J = 8.8 Hz, 2H), 6.66 (d, J = 8.8 Hz, 2H), 6.38 (d, J = 3.6 Hz, 1H), 5.11 (dt, J = 13.5, 6.8 Hz, 1H), 3.74 (s, 1H), 2.86 (s, 3H), 1.52 (d, J = 6.8 Hz, 6H); ^{13}C NMR (100 MHz, CDCl_3) δ 163.0, 151.9, 150.6, 147.0, 144.0, 122.5, 122.4, 112.9, 105.4, 98.6, 46.1, 30.9, 22.7; HRMS $[\text{M}]^+$ calcd for $\text{C}_{16}\text{H}_{18}\text{N}_4\text{O}$ 282.1481, found 282.1484. The purity of the compound was >99% by HPLC.

4.1.25. 7-Isopropyl-4-(4-dimethylaminophenoxy)-7H-pyrrolo[2,3-d]pyrimidine (4b)

Off white solid (41%); ^1H NMR (300 MHz, CDCl_3) δ 8.45 (s, 1H), 7.16 (d, J = 3.6 Hz, 1H), 7.11 (d, J = 9.0 Hz, 2H), 6.78 (d, J = 9.0 Hz, 2H), 6.39 (d, J = 3.6 Hz, 1H), 5.11 (dt, J = 13.5, 6.8 Hz, 1H), 2.97 (s, 6H), 1.52 (d, J = 6.8 Hz, 6H); ^{13}C NMR (100 MHz, d_6 -DMSO) δ 163.0, 151.9, 150.6, 148.4, 143.6, 122.5, 122.2, 113.3, 105.5, 98.6, 46.1, 40.9, 22.7; HRMS $[\text{M}]^+$ calcd for $\text{C}_{17}\text{H}_{20}\text{N}_4\text{O}$ 296.1637, found 296.1635. The purity of the compound was >95% by HPLC.

4.1.26. 7-(2-Methylallyl)-4-(4-methylaminophenoxy)-7H-pyrrolo[2,3-d]pyrimidine (4c)

Yellow solid (22%); ^1H NMR (300 MHz, CDCl_3) δ 8.46 (s, 1H), 7.07 (d, J = 8.9 Hz, 2H), 7.04 (d, J = 3.5 Hz, 1H), 6.65 (d, J = 8.9 Hz, 2H), 6.42 (d, J = 3.5 Hz, 1H), 4.92 (s, 1H), 4.78 (s, 2H), 4.68 (s, 1H), 3.80 (s, 1H), 2.84 (s, 3H), 1.70 (s, 3H); ^{13}C NMR (100 MHz, CDCl_3) δ 163.1, 152.7, 151.1, 147.0, 143.9, 140.9, 126.2, 122.4, 112.9, 105.2, 98.9, 50.1, 30.9, 19.8; HRMS $[\text{M}]^+$ calcd for $\text{C}_{17}\text{H}_{18}\text{N}_4\text{O}$ 294.1481, found 294.1486. The purity of the compound was >95% by HPLC.

4.1.27. 7-(2-Methylallyl)-4-(4-dimethylaminophenoxy)-7H-pyrrolo[2,3-d]pyrimidine (4d)

Off white solid (39%); ^1H NMR (300 MHz, CDCl_3) δ 8.47 (s, 1H), 7.12 (d, J = 9.1 Hz, 2H), 7.04 (d, J = 3.5 Hz, 1H), 6.78 (d, J = 9.1 Hz, 2H), 6.43 (d, J = 3.5 Hz, 1H), 4.93 (s, 1H), 4.79 (s, 2H), 4.68 (s, 1H), 2.96 (s, 6H), 1.71 (s, 3H); ^{13}C NMR (100 MHz, CDCl_3) δ 163.1, 152.7, 151.1, 148.5, 143.6, 140.9, 126.2, 122.1, 113.3, 112.8, 105.2, 98.9, 50.1, 40.9, 19.9; HRMS $[\text{M}]^+$ calcd for $\text{C}_{18}\text{H}_{20}\text{N}_4\text{O}$ 308.1637, found 308.1645. The purity of the compound was >99% by HPLC.

4.2. Biology: Material and methods

D-Luciferin sodium salt (L6882), adenosine 5'-triphosphate disodium (ATP) (A7699), and luciferase (*Photinus pyralis*) (L9506) were purchased from Sigma-Aldrich (St. Louis, MO, USA). Bovine serum albumin (BSA, fraction V) was from Biowest (Miami, Florida, USA). All other chemicals were obtained from standard commercial sources. A stock solution of luciferase was prepared by dissolving the lyophilized powder in buffer A (1 M glycine-Tris buffer containing 10 mM EDTA and 100 mM MgSO_4 , pH 7.8) (320 nM luciferase) and stored in small aliquots at -80°C . D-luciferin and ATP

were prepared in buffer B (50 mM glycine-Tris buffer supplemented with 5 mM MgSO_4 , 0.5 mM EDTA, 0.1% (w/v) BSA, pH 7.8) at 2 mM and 900 μM , respectively, as stock solution and stored at -80°C .

All the enzyme reactions took place at room temperature and were performed at least in triplicate. The bioluminescence tests were performed in a flexstation 3 Microplate Reader (Molecular Devices, Sunnyvale, CA, USA) in flex mode according to a slightly modified protocol from Sigma-Aldrich (EC 1.13.12.7). Briefly, inhibition assays were performed using 32 nM firefly luciferase in buffer A, 50 μM D-luciferin and 250 μM ATP in buffer B, and incubated with either a single concentration of inhibitor (10 μM) or different concentrations of inhibitor. Inhibition kinetics of luciferase assays with respect to D-luciferin were performed using different concentrations of D-luciferin (3.125–200 μM), where the ATP concentration was fixed at 250 μM . Inhibition kinetics of luciferase assays with respect to ATP were performed under equal conditions, where the ATP concentration varied from 25 to 500 μM and the concentration of D-luciferin was fixed at 50 μM . Typically, a well containing 10 μL of buffer B or inhibitor, and 10 μL of luciferase solution were mixed and incubated for 20 min in the dark at room temperature. Then, 80 μL of D-luciferin/ATP solution was injected; emitted light was integrated in 1 ms and recorded in 0.8 s intervals for 46 s. The peak signal was read as the initial velocity of catalyzed reaction by luciferase. All the indicated concentrations refer to the final volume of 100 μL .

4.2.1. Data analysis

All data were analyzed using the GraphPad Prism 5.01 software (GraphPad Software Inc., San Diego, CA, USA). Half of the inhibitory concentration of compound (IC_{50}) was directly obtained from the concentration-effect curves fitting with log (inhibitors) vs normalized response method. The K_m^{app} and $V_{\text{max}}^{\text{app}}$ values of luciferase for D-luciferin and ATP in the absence or presence of **3a** were obtained from a nonlinear fit analysis of the enzyme kinetics curve with the Michaelis–Menten model. The dissociation constant value (K_i or αK_i) of inhibitor and the K_m and V_{max} values of luciferase were directly obtained from the nonlinear regression analysis of the enzyme kinetics curve with a mixed or uncompetitive inhibition model.

4.2.2. Docking studies

Molecular docking was carried out by software Autodock4.³⁴ The X-ray structure of firefly luciferase (from *Photinus pyralis*) inhibitor complex (PDB code: 3IES³⁵) was retrieved from the Protein Data Bank (<http://www.rcsb.org/pdb>) for docking calculations. The active site was defined by a grid box as large as $70 \times 70 \times 70$ points with grid spacing of 0.375 Å using AutoGrid4. The box was centered on the center of the molecule PTC124-AMP in the crystal structure. The Lamarckian genetic algorithm was applied to account for protein-ligand interactions. Finally, the conformation with the lowest predicted binding free energy of the most occurring binding modes in the firefly luciferase active pocket was selected.

Acknowledgments

This work was supported by State key Laboratory of Drug Research and National Science Fund for Distinguished Young Scholars (81125025) in China.

Supplementary data

Supplementary data associated with this article can be found, in the online version, at <http://dx.doi.org/10.1016/j.bmc.2012.07.035>.

References and notes

1. Inouye, S. *Cell Mol. Life Sci.* **2010**, *67*, 387.
2. Marques, S. M.; da Silva, Esteves J.C. *IUBMB Life* **2009**, *61*, 6.
3. Fraga, H. *Photochem. Photobiol. Sci.* **2008**, *7*, 146.
4. Leitao, J. M.; Esteves da Silva, J. C. J. *Photochem. Photobiol. B* **2010**, *101*, 1.
5. Bedford, R.; LePage, D.; Hoffmann, R.; Kennedy, S.; Gutschenritter, T.; Bull, L.; Sujijantarat, N.; DiCesare, J. C.; Sheaff, R. J. *Photochem. Photobiol. B* **2012**, *107*, 55.
6. Green, A. A.; McElroy, W. D. *Biochim. Biophys. Acta* **1956**, *20*, 170.
7. de Wet, J. R.; Wood, K. V.; Helinski, D. R.; DeLuca, M. *Proc. Natl. Acad. Sci. U.S.A.* **1985**, *82*, 7870.
8. Naylor, L. H. *Biochem. Pharmacol.* **1999**, *58*, 749.
9. Fan, F.; Wood, K. V. *Assay Drug Dev. Technol.* **2007**, *5*, 127.
10. Michelini, E.; Cevenini, L.; Mezzanotte, L.; Coppa, A.; Roda, A. *Anal. Bioanal. Chem.* **2010**, *398*, 227.
11. Inglese, J.; Johnson, R. L.; Simeonov, A.; Xia, M.; Zheng, W.; Austin, C. P.; Auld, D. S. *Nat. Chem. Biol.* **2007**, *3*, 466.
12. Thorne, N.; Inglese, J.; Auld, D. S. *Chem. Biol.* **2010**, *17*, 646.
13. Auld, D. S.; Southall, N. T.; Jadhav, A.; Johnson, R. L.; Diller, D. J.; Simeonov, A.; Austin, C. P.; Inglese, J. *J. Med. Chem.* **2008**, *51*, 2372.
14. Fetzner, S.; Steiner, R. A. *Appl. Microbiol. Biotechnol.* **2010**, *86*, 791.
15. Danielson, P. B. *Curr. Drug. Metab.* **2002**, *3*, 561.
16. Fontanesi, F.; Soto, I. C.; Horn, D.; Barrientos, A. *Am. J. Physiol. Cell Physiol.* **2006**, *291*, C1129.
17. Edmondson, D. E.; Mattevi, A.; Binda, C.; Li, M.; Hubalek, F. *Curr. Med. Chem.* **1983**, *2004*, 11.
18. Sudhaharan, T.; Reddy, A. R. *Biochemistry* **1998**, *37*, 4451.
19. da Silva, L. P.; da Silva, J. C. *Photochem. Photobiol. Sci.* **2011**, *10*, 1039.
20. Lemasters, J. J.; Hackenbrock, C. R. *Biochemistry* **1977**, *16*, 445.
21. Ribeiro, C.; Esteves da Silva, J. C. *Photochem. Photobiol. Sci.* **2008**, *1085*, 7.
22. Szarecka, A.; Xu, Y.; Tang, P. *Biophys. J.* **2007**, *1895*, 93.
23. Auld, D. S.; Zhang, Y. Q.; Southall, N. T.; Rai, G.; Landsman, M.; MacLure, J.; Langevin, D.; Thomas, C. J.; Austin, C. P.; Inglese, J. *J. Med. Chem.* **2009**, *52*, 1450.
24. Takehara, K.; Kamaya, H.; Ueda, I. *Biochim. Biophys. Acta* **2005**, *1721*, 124.
25. Welsch, M. E.; Snyder, S. A.; Stockwell, B. R. *Curr. Opin. Chem. Biol.* **2010**, *14*, 347.
26. Lee, J. H.; Lim, H. S. *Org. Biomol. Chem.* **2012**, *10*, 4229.
27. Fang, J. P.; Liu, Y.; Li, J.; Liao, W. F.; Hu, Y. H.; Ding, K. *Acta Pharmacol. Sin.* **2012**. <http://dx.doi.org/10.1038/aps.2012.56>.
28. Lambert, N.; Idahl, L. A. *Biochem. J.* **1995**, *305*, 929.
29. Heitman, L. H.; van Veldhoven, J. P.; Zweemer, A. M.; Ye, K.; Brussee, J.; AP, I. J. *J. Med. Chem.* **2008**, *51*, 4724.
- [30]. McHardy, T.; Caldwell, J. J.; Cheung, K. M.; Hunter, L. J.; Taylor, K.; Rowlands, M.; Ruddle, R.; Henley, A.; de Haven Brandon, A.; Valenti, M.; Davies, T. G.; Fazal, L.; Seavers, L.; Raynaud, F. I.; Eccles, S. A.; Aherne, G. W.; Garrett, M. D.; Collins, I. *J. Med. Chem.* **2010**, *53*, 2239.
31. Thoma, G.; Nuninger, F.; Falchetto, R.; Hermes, E.; Tavares, G. A.; Vangrevelinghe, E.; Zerwes, H. G. *J. Med. Chem.* **2011**, *54*, 284.
32. Wu, R.; Smidansky, E. D.; Oh, H. S.; Takhampunya, R.; Padmanabhan, R.; Cameron, C. E.; Peterson, B. R. *J. Med. Chem.* **2010**, *53*, 7958.
33. Hu, W.; Wang, P.; Song, C.; Pan, Z.; Wang, Q.; Guo, X.; Yu, X.; Shen, Z.; Wang, S.; Chang, J. *Bioorg. Med. Chem. Lett.* **2010**, *20*, 7297.
34. Morris, G. M.; Goodsell, D. S.; Halliday, R. S.; Huey, R.; Hart, W. E.; Belew, R. K.; Olson, A. J. *J. Comput. Chem.* **1998**, *19*, 1639.
35. Auld, D. S.; Lovell, S.; Thorne, N.; Lea, W. A.; Maloney, D. J.; Shen, M.; Rai, G.; Battaile, K. P.; Thomas, C. J.; Simeonov, A.; Hanzlik, R. P.; Inglese, J. *Proc. Natl. Acad. Sci. U.S.A.* **2010**, *107*, 4878.